Self-Assembly

Deutsche Ausgabe: DOI: 10.1002/ange.201701978
Internationale Ausgabe: DOI: 10.1002/anie.201701978

Toroid Formation through a Supramolecular "Cyclization Reaction" of Rodlike Micelles

Chaoying Yang[+], Liang Gao[+], Jiaping Lin, Liquan Wang, Chunhua Cai,* Yuhan Wei, and Zhibo Li*

Abstract: *Constructing polymeric toroids with a uniform, tunable size is challenging. Reported herein is the formation of uniform toroids from poly(γ-benzyl-L-glutamate)-graft-poly(ethylene glycol) (PBLG-g-PEG) graft copolymers by a two-step self-assembly process. In the first step, uniform rodlike micelles are prepared by dialyzing the polymer dissolved in tetrahydrofuran (THF)/N,N′-dimethylformamide (DMF) against water. With the addition of THF in the second step, the rodlike micelles curve and then close end-to-end to form uniform toroids, which resemble a cyclization reaction.*

Toroidal structures have attracted considerable interest in nanoscience because of their rarity, complexity, and unique configuration.[1] Studies on these structures can be important for understanding a number of biological processes, such as the toroidal condensation of DNA, and for guiding the design of new bioinspired nanostructures for gene delivery.[2] Macromolecular self-assembly allows construction of a variety of supramolecular aggregates, including toroidal structures.[3] Polymeric toroids can be prepared in two general ways.[4] One is that toroids are formed by a complex self-assembly process.[4f,g] While, in the other way, toroids are formed by end-to-end closure of rodlike assemblies initially formed in solution. However, this end-to-end closure process is usually accompanied by the end-to-end connection of two different rods to form jointed rods, which is due to the small energy difference between the two states. In addition, these longer rods may further close into toroids. As a result, in these systems, the toroids are accompanied by rods and usually exhibit a wide size distribution.[4a,b,f] Preparing pure toroids with a uniform and tunable size remains a challenge.

Recently, some research groups have found that the self-assembly of building blocks, including polymers,[5] polymer assemblies,[6] and nanocrystals,[7] can result in aggregation in a manner analogous to the polymerization of unimers into polymers. For example, our group reported that anisotropic spindle-like micelles, self-assembled from polypeptide graft copolymers with rigid backbones, can connect end-to-end and grow into one-dimensional nanowires in a manner that resembles step polymerization.[8] Based on this impressive body of work using polymer aggregates as building blocks to construct nanostructures, and considering that the end-to-end closure of a molecule is an efficient method to produce rings,[9] we envisaged that the end-to-end closure of preassembled rodike micelles could be an attractive method for preparing toroids.

Herein, we report the formation of uniform toroids in aqueous solution using end-to-end closure of preassembled rodlike micelles constructed from polypeptide-based graft copolymers (PBLG-*g*-PEG). Firstly (Step 1), uniform rodlike micelles (also termed spindle-like micelles), which are approximately 600 nm in length, were prepared by adding water to a THF/DMF solution of polymers, and then dialyzing the mixture against water at 30 °C (Figure 1 a). In the rodlike micelles, the rigid PBLG backbones should align with each other, with their direction parallel to the axial direction of the rods.[8,10] In Step 2, a certain amount of THF is added to the solution of rodlike micelles to induce the self-assembly. After

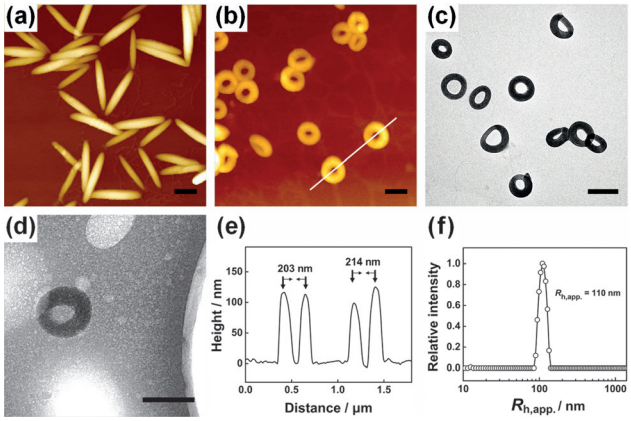

Figure 1. a) AFM image of rodlike micelles self-assembled from PBLG-*g*-PEG copolymers in Step 1. b) AFM, c) TEM, and d) cryo-TEM images of toroids self-assembled from rodlike micelles with the addition of 55.6 vol% THF at 30 °C in Step 2. e) AFM height profile along the white line in (b). f) Apparent hydrodynamic radius ($R_{h,app.}$) distribution of toroids in water at a scattering angle of 90°. Scale bars: 300 nm. Here, the molecular weight of the PBLG backbone and PEG is 300 000 and 750, respectively. The grafting degree of PEG is 0.19%. More detailed information regarding the characteristics of the polymers is provided in the Supporting Information (Table S1).

[*] C. Yang,[+] L. Gao,[+] Prof. Dr. J. Lin, Dr. L. Wang, Dr. C. Cai
Shanghai Key Laboratory of Advanced Polymeric Materials
School of Materials Science and Engineering
East China University of Science and Technology
Shanghai 200237 (China)
E-mail: jlin@ecust.edu.cn
caichunhua@ecust.edu.cn
Homepage: http://jlinlab.ecust.edu.cn/
Dr. Y. Wei, Prof. Dr. Z. Li
School of Polymer Science and Engineering
Qingdao University of Science and Technology
Qingdao 266042 (China)
[+] These authors contributed equally to this work.

Supporting information for this article can be found under: http://dx.doi.org/10.1002/anie.201701978.

stabilization at 30 °C for 24 hours, the aggregate solution was dialyzed against water to remove the THF. Experimental details are available in Sections 1.1–1.4 of the Supporting Information. As shown in the atomic force microscopy (AFM) and TEM images in Figures 1 b and c, uniformly sized toroidal structures were formed in Step 2. The corresponding cryo-TEM image (Figure 1 d) reveals the same morphology, thus the effect of drying on sample preparations can be ruled out. The AFM height profile shows that the diameter of the toroid (D_{toroid}) is approximately 205 nm (Figure 1 e), thus the corresponding circumference of the toroid (C_{toroid}) is approximately 644 nm, which is close to the length of the rodlike micelles (L_{rod}) in Figure 1 a. In addition, Figure 1 f displays a narrow apparent hydrodynamic radius ($R_{h,app.}$) distribution with $R_{h,app.} =$ 110 nm, which indicates the uniform size of toroids. The details of the size comparison between the rodlike micelles and toroids are presented in the Supporting Information (see Section 1.5 and Figure S2). The toroid formation can reasonably be attributed to the ring-closure of the rodlike micelles.

To gain insight into the role of THF in the formation of the toroids in Step 2, we examined the effect of the added amount of THF on the resulting morphology. The results are presented in Figure 2. When 20.0 vol % of THF was added (i.e., the volume percentage of the added THF relative to the whole volume), the rodlike micelles (Figure 2 a) curved with a small bending degree (Figure 2 b). The bending degree is reflected by the bend angle of the curved rods (φ) and is defined as the supplementary angle of the angle between the two straight lines formed by connecting the midpoint and the ends of the curved rod (illustrated in the inset of Figure 2 f). Upon further increasing the THF content, the bending degree of the curved rods continues to increase (Figure 2 c,d). When the THF content reaches 50.0 vol%, the two ends of the rods meet and form toroids (Figure 2 e). Interestingly, the connection junctions of some toroids are clearly visible (insets in Figure 2 e). When the THF content is increased to 55.6 vol %, these junctions disappear, and perfect toroidal structures are obtained, as shown in Figure 1 b,c and d. The morphology transition was also confirmed by cryo-TEM results, which rules out drying effects from the sample preparations (see Figure S4). We also examined the stability of the formed aggregates. The storage time had a negligible effect on the morphologies of the curved rods and toroids (see Figure S5). To gain an in-depth understanding of the effect of the solvent, we plotted φ as a function of the THF content, and the results are illustrated in Figure 2 f. The average φ value was obtained by measuring more than 200 micelles for each sample (see Figure S6). As shown in the figure, the bend angle continuously increases with the increasing amount of THF. When the THF content reaches 55.6 vol % or more, the bend angle reaches 180°, which corresponds to the formation of toroids.

Temperature is an important factor in determining self-assembly structures.[4e,10b] We examined the effect of the self-assembling temperature on the toroid formation in Step 2. After the addition of THF, the aggregate morphology in the THF/water solvent is sensitive to temperature before they are frozen by dialysis. We first prepared a group of samples by adding 55.6 vol % of THF to the solution of rodlike micelles at 15 °C. Then, the temperature was increased to 20, 25, and 30 °C to anneal the samples for 24 hours. The sample at 15 °C maintained its rod shape (Figure 3 a). When the temperature increased, the rods curved, and the bending degree increases with temperature, finally toroids were formed (Figures 3 b–d). This behavior is similar to the observed dependence of the bend angle φ on the THF content. As shown in Figure 3 e (red solid line), the bend angle φ increased with the increasing temperature from 15 to 30 °C. The toroids were obtained at 30 °C. These toroids were stable in the temperature range from 30 to 40 °C. When the temperature was higher than 40 °C, the toroids collapsed (see Figure S7).

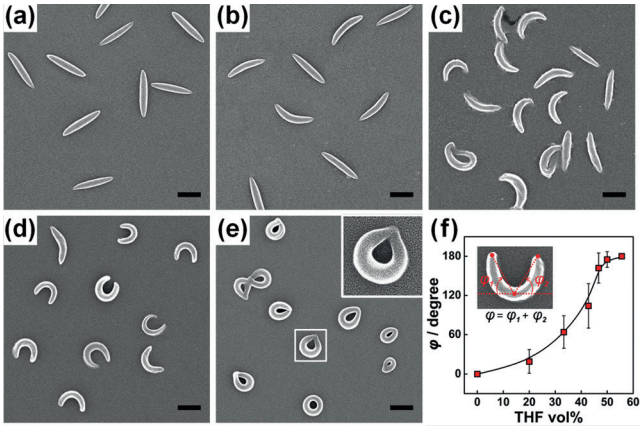

Figure 2. a–e) SEM images of the aggregates self-assembled from rodlike micelles with various amounts of THF added to the aqueous solution of rodlike micelles: a) 0 vol %, b) 20.0 vol %, c) 33.3 vol %, d) 42.8 vol %, and e) 50.0 vol %. f) Variation in bend angle φ as a function of THF content. Inset is the definition of bend angle φ. The experimental temperature was fixed at 30 °C. After addition of THF, the solution was stabilized for 24 hours to achieve equilibrium. Scale bars: 300 nm.

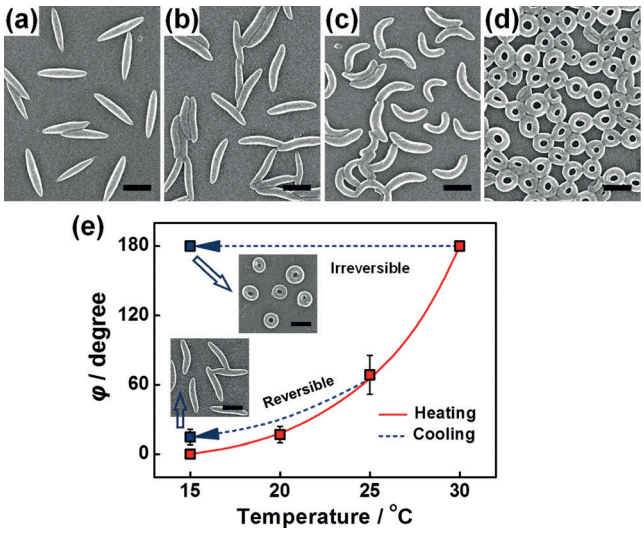

Figure 3. a–d) SEM images of the aggregates self-assembled from rodlike micelles with various annealing temperatures: a) 15 °C, b) 20 °C, c) 25 °C, and d) 30 °C. e) Variation in the bend angle φ as a function of temperature. Insets in (e) show the SEM images of the corresponding samples cooled to 15 °C. Scale bars: 300 nm.

Further studies revealed that the rod-to-curved-rod morphology transition is reversible with a change in the temperature if it was not frozen by dialysis. As illustrated in Figure 3e (blue dotted line), when the samples annealed at 25 °C were cooled to 15 °C, the curved rods (Figure 3c, $\varphi = 68.5°$) converted into straight rods (lower inset in Figure 3e, $\varphi = 14.6°$). However, the formed toroids annealed at 30 °C (Figure 3d, $\varphi = 180°$) did not change (upper inset in Figure 3e, $\varphi = 180°$) when the sample was cooled to 15 °C. These structures were maintained because the end caps of the rodlike micelles were connected through physical bonding of the PBLG chains (more details in the following section). In addition, the effect of the grafting degree on the self-assembled structures was also examined. When the grafting degree of the PEG was relatively high, the preformed rodlike micelles tended to transform into spheres rather than toroids in Step 2 (see Figure S8). More importantly, controlling the size of the toroids is usually difficult.[3a,4a–f] However, for the two-step self-assembly process in this work, the size of the toroids depends on the length of the initially formed rods, which can be regulated by the molecular weight of the PBLG backbone of the graft copolymers. We found that the circumference of the toroid is dependent on the molecular weight of the PBLG. A higher molecular weight led to a larger circumference, which implies that the size of the toroid can be effectively controlled (see Figure S9).

PBLG molecules are well known to be highly soluble in DMF, in which phenyl-substituents on PBLG backbone (abbreviated as pendant groups) have a relatively extended packing form resulting from the strong interactions between the solvent and the pendant groups.[10b,11] In Step 1, the pendant groups could pack in a relatively extended manner in DMF/THF and be preserved by dialysis. When THF was added in Step 2, the interaction between the solvents and the pendant groups weakened as THF is not a good solvent,[10c,11c] and the PBLG side chains shrank accordingly. This behavior could generate higher interfacial energy between the micelle core and shell. In response, the rodlike micelles tend to collapse into compact spheres to reduce the higher interfacial energy. However, because of the rigid nature of the rodlike micelles, toroids formed instead of collapsed spheres.[3d,4a–c,12] Moreover, because of the anisotropic nature of the rodlike micelles, the two ends of the rod are not covered well by PEG and a higher energy could be generated when THF is added.[8] This could result in "reactive points" at the ends, thus accelerating toroid formation. The process behaves similarly to a cyclization reaction but takes place at the supramolecular level. Note that the end-cap energy could drive one-dimensional growth of the rodlike micelles through the fusion of the micelle ends if no unfavorable interfacial energy exists.[8]

To verify our speculation that the packing mode of the pendant groups changes in the rod-to-toroid morphology transition, we performed circular dichroism (CD) experiments for the aggregates prepared under various solvent and temperature conditions, and their spectra are presented in Figures 4a and b. As shown in the figure, all the spectra show double peaks in the negative region at approximately $\lambda = 200$–220 nm, which indicates the α-helix conformation of the PBLG backbone (the α-helix conformation was also confirmed by FTIR; see Figure S10). The packing mode of the pendant groups is indicated by the band in the $\lambda = 230$–280 nm region of the CD spectra. A positive band indicates a shrunken left-handed arrangement of the pendant groups, while a negative band corresponds to a loose right-handed form.[10b,11] The magnitude of the band characterizes the packing regularity of the pendant groups, that is, the more shrunken the pendant groups are, the more obvious the positive band is.[11a] As shown in Figure 4a, a positive band is seen for the rodlike micelle solution without THF, which indicates a relatively extended left-handed form. When THF is added, the intensity of this band increases, thus suggesting that the pendant group packing is more constricted.[11a] As the THF content increases, the pendant group band becomes more prominent. This data indicates a highly shrunken packing form of the pendant groups. The chiral arrangement of the pendant groups is also related to the temperature. Figure 4b shows the CD results for the samples at various temperatures after they were dialyzed. The band intensity of the left-handed pendant groups increases with the temperature, and indicates that the pendant groups shrank at higher temperatures. The results indicate that both the THF-rich and higher temperature environments could lead to the constriction of the pendant groups. This constriction would increase the unfavorable interfacial energy and drive the formation of toroids.

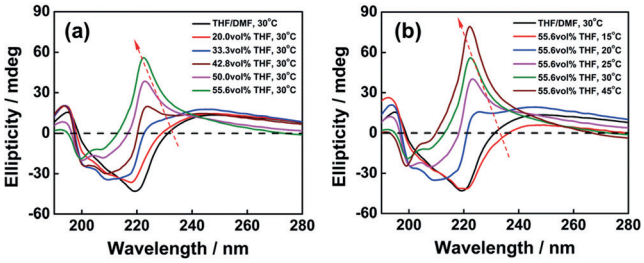

Figure 4. CD spectra of PBLG-*g*-PEG aggregates formed in Step 2 as a function of organic solvents and temperature conditions: a) various THF contents, 30 °C; b) 55.6 vol% THF, various temperatures. The black line represents the rodlike micelles formed in Step 1. The changes of the chiral packing bands of pendant groups are guided by red arrows.

To further understand the two-step self-assembly mechanism, we performed Brownian dynamics (BD) simulations to examine the rod-to-toroid morphology transition of the aggregates (simulation details are given in Section 2 of the Supporting Information).[13] For this purpose, we constructed a coarse-grained model of the graft copolymer with a rigid backbone, pendant groups, and side chains to represent the rigid PBLG backbone, pendant groups on PBLG backbone, and the grafted PEG chains, respectively (Figure 5a). The modeled copolymers self-assembled into rodlike micelles at the interaction parameters $\varepsilon_{RR} = \varepsilon_{PP} = 1.2\,\varepsilon$ (Figure 5b), and is consistent with the self-assembly occurring in Step 1. The simulations revealed that the rigid backbones arrange themselves in parallel with the long axis of the rodlike micelle, and the imperfect coverage of the grafted side chains at the two ends leads to structural defects (see Figure S12). To simulate

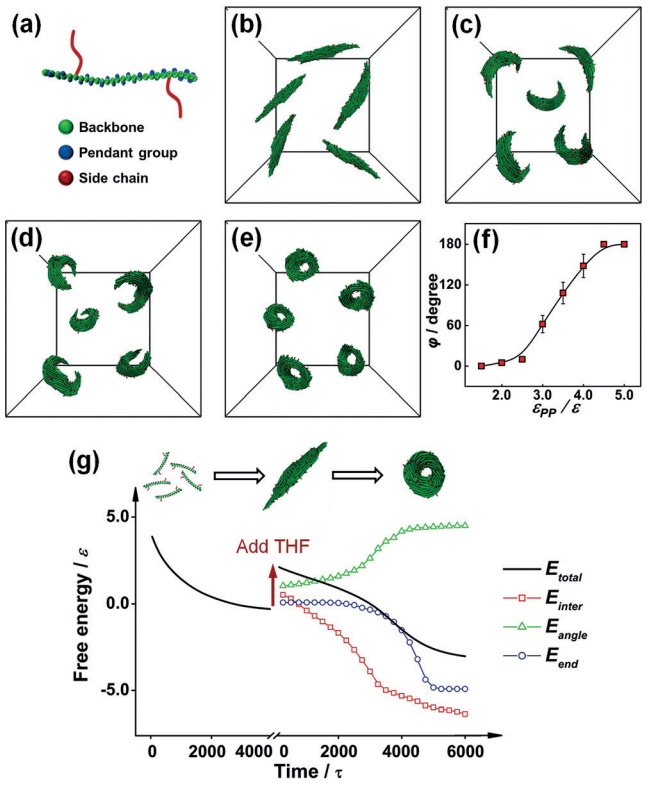

Figure 5. a) Coarse-grained model of a rod-*g*-coil graft copolymer with a rigid backbone (green), pendant groups (blue), and side chains (red). b) Simulated rodlike micelles self-assembled at $\varepsilon_{RR}=\varepsilon_{PP}=1.2\,\varepsilon$. c,d) Curved micelles bended from rodlike micelles when ε_{PP} was increased to $3.0\,\varepsilon$ and $4.0\,\varepsilon$, respectively. e) Toroidal micelles transformed from rodlike micelles when ε_{PP} was increased to $5.0\,\varepsilon$. f) Variation in the bend angle φ as a function of ε_{PP}. g) Free-energy change as a function of the simulation time for the two-step self-assembly.

the Step 2, we increased the interaction parameter, ε_{PP}, which simulates the increasing unfavorable interfacial energy between the micelle core and shell caused by adding THF. If we increase the ε_{PP} step by step to represent adding various amounts of THF to the solution, curved micelles with different bending degrees are obtained (Figures 5 c,d). Under a stronger interaction of $\varepsilon_{PP}=5.0\varepsilon$, the toroidal micelles formed completely (Figure 5 e). The bend angle φ increased from 0 to 180°, as shown in Figure 5 f. The structural characteristics of the toroids are presented in the Supporting Information (Section 2.4; Figure S13). The simulation results well reproduced the morphology transition seen in the experiments.

To gain insight into the driving force for the two-step self-assembly, we calculated the free-energy changes in the self-assembly process. The free-energy (E_{total}) change can be divided into three parts, that is, the change in the interfacial energy (E_{inter}), the bending energy of the rods (E_{angle}), and the end-cap energy (E_{end}). The calculation results for these energy changes in the two-step self-assembly are plotted in Figure 5 g (the calculation details are available in Section 2.2.8 of the Supporting Information). In Step 1, the rod-*g*-coil graft copolymers self-assemble into rodlike micelles. As a result, the total potential energy, E_{total}, decreases and reaches an equilibrium state, and indicates that the rodlike micelles are stable structures. Upon the addition of THF in Step 2, the solubility and packing mode of the pendant groups change in response to the change in the solvent environment, and results in a higher E_{inter} value. Meanwhile, because of the structure defects at both ends, the addition of THF could give rise to higher E_{end} values at both ends of the rod micelles. At this point, the rods are far from equilibrium (i.e., a higher E_{total}; see the red arrow in Figure 5 g). To reduce the E_{inter} value and achieve equilibrium, the rodlike micelles tend to self-assemble into curved rods by bending the rigid micelles. This process leads to an increase in the bending energy, E_{angle}. However, because of the high-energy defects at both ends of the rods, the end-to-end connection of the curved rods significantly reduces the E_{end} value. Eventually, the interplay of the three parts of the free energy changes leads to a new equilibrium for the toroids. Note that the rigidity of the micelles prevents the toroids from collapsing into spheres. If the polymer backbone is not sufficiently rigid, collapsed spheres are obtained (see Figure S14). Indeed, we observed collapsed spheres or collapsed toroids if the PBLG rigidity was decreased by grafting more PEG or by increasing the temperature (note that for the temperature-induced collapse, in addition to the chain softening upon increasing the temperature, the constriction of the side chains also contributes to the collapse of the toroid; see Figures S7, S8). The mechanism wherein the rigidity of the rods sustains the toroidal structure is firmly supported by the simulation.

The end-to-end closure of rodlike micelles observed in this work is an unprecedented finding. This process is not unlike the cyclization reaction, but it occurs at a supramolecular level. The gained information may provide useful guidance in understanding some biological process, such as DNA condensation where high-molecular-weight DNA molecules produce toroidal bundles with higher ordered local chain packing.[2a] Both the toroids are formed from rodlike building blocks, and the rigid (with some flexibility) nature of both DNA molecules and rodlike micelles is important for forming the toroids but not collapse into spherical structures.

In summary, we discovered the formation of toroids through end-to-end closure of rodlike micelles in a process resembling cyclization of the molecule into rings. The PBLG-*g*-PEG graft copolymers first self-assemble into rodlike micelles in an aqueous solution. The rods curved and then connected end-to-end to form toroids upon adding THF. The cyclization of the rodlike micelles can also be achieved by increasing the temperature. This THF- and temperature-induced rod-to-toroid transition was found to be associated with the variation in the arrangement of the side chains on the PBLG backbone. The mechanism governing the end-to-end connection of the rods into toroids enables controlling the size of the toroids using the length of the initial rodlike micelles.

Acknowledgments

This work was supported by the National Natural Science Foundation of China (21234002, 21474029, and 51573049).

Conflict of interest

The authors declare no conflict of interest.

Keywords: cyclizations · polymers · polypeptide · theoretical simulation · toroidal structures

How to cite: *Angew. Chem. Int. Ed.* **2017**, *56*, 5546 – 5550
Angew. Chem. **2017**, *129*, 5638 – 5642

[1] a) Y. Kim, W. Li, S. Shin, M. Lee, *Acc. Chem. Res.* **2013**, *46*, 2888 – 2897; b) D. Presa-Soto, G. A. Carriedo, R. de la Campa, A. Presa Soto, *Angew. Chem. Int. Ed.* **2016**, *55*, 10102 – 10107; *Angew. Chem.* **2016**, *128*, 10256 – 10261.

[2] a) V. A. Bloomfield, *Biopolymers* **1997**, *44*, 269 – 282; b) D. Luo, W. M. Saltzman, *Nat. Biotechnol.* **2000**, *18*, 893 – 895; c) A. P. Rolland, *Crit. Rev. Ther. Drug Carrier Syst.* **1998**, *15*, 143 – 198.

[3] a) H. Huang, B. Chung, J. Jung, H.-W. Park, T. Chang, *Angew. Chem. Int. Ed.* **2009**, *48*, 4594 – 4597; *Angew. Chem.* **2009**, *121*, 4664 – 4667; b) L. Chen, T. Jiang, J. Lin, C. Cai, *Langmuir* **2013**, *29*, 8417 – 8426; c) S. J. Holder, N. A. J. M. Sommerdijk, *Polym. Chem.* **2011**, *2*, 1018 – 1028; d) X. Li, Y. Gao, X. Xing, G. Liu, *Macromolecules* **2013**, *46*, 7436 – 7442; e) H. Luo, J. L. Santos, M. Herrera-Alonso, *Chem. Commun.* **2014**, *50*, 536 – 538; f) C. Luo, Y. Liu, Z. Li, *Soft Matter* **2012**, *8*, 2618 – 2626; g) D. Li, X. Jia, X. Cao, T. Xu, H. Li, H. Qian, L. Wu, *Macromolecules* **2015**, *48*, 4104 – 4114.

[4] a) D. J. Pochan, Z. Chen, H. Cui, K. Hales, K. Qi, K. L. Wooley, *Science* **2004**, *306*, 94 – 97; b) H. Cui, Z. Chen, K. L. Wooley, D. J. Pochan, *Soft Matter* **2009**, *5*, 1269 – 1278; c) X. Li, M. Deng, Y. Liu, H. Liang, *J. Phys. Chem. B* **2008**, *112*, 14762 – 14765; d) C. Liu, G. Chen, H. Sun, J. Xu, Y. Feng, Z. Zhang, T. Wu, H. Chen, *Small* **2011**, *7*, 2721 – 2726; e) Z. Wang, W. Jiang, *Soft Matter* **2010**, *6*, 3743 – 3746; f) H. Yu, W. Jiang, *Macromolecules* **2009**, *42*, 3399 – 3404; g) X. He, F. Schmid, *Phys. Rev. Lett.* **2008**, *100*, 137802.

[5] a) Y. Huang, Y. Mai, X. Yang, U. Beser, J. Liu, F. Zhang, D. Yan, K. Müllen, X. Feng, *J. Am. Chem. Soc.* **2015**, *137*, 11602 – 11605; b) A. Presa Soto, J. B. Gilroy, M. A. Winnik, I. Manners, *Angew. Chem. Int. Ed.* **2010**, *49*, 8220 – 8223; *Angew. Chem.* **2010**, *122*, 8396 – 8399.

[6] a) X. Yan, G. Liu, Z. Li, *J. Am. Chem. Soc.* **2004**, *126*, 10059 – 10066; b) A. H. Gröschel, F. H. Schacher, H. Schmalz, O. V. Borisov, E. B. Zhulina, A. Walther, A. H. E. Müller, *Nat. Commun.* **2012**, *3*, 710; c) H. Cui, Z. Chen, S. Zhong, K. L. Wooley, D. J. Pochan, *Science* **2007**, *317*, 647 – 650.

[7] a) K. Liu, Z. Nie, N. Zhao, W. Li, M. Rubinstein, E. Kumacheva, *Science* **2010**, *329*, 197 – 200; b) L. J. Hill, N. Pinna, K. Char, J. Pyun, *Prog. Polym. Sci.* **2015**, *40*, 85 – 120.

[8] Z. Zhuang, T. Jiang, J. Lin, L. Gao, C. Yang, L. Wang, C. Cai, *Angew. Chem. Int. Ed.* **2016**, *55*, 12522 – 12527; *Angew. Chem.* **2016**, *128*, 12710 – 12715.

[9] G. Polymeropoulos, P. Bilalis, N. Hadjichristidis, *ACS Macro Lett.* **2016**, *5*, 1242 – 1246.

[10] a) C. Cai, J. Lin, Y. Lu, Q. Zhang, L. Wang, *Chem. Soc. Rev.* **2016**, *45*, 5985 – 6012; b) C. Cai, J. Lin, X. Zhu, S. Gong, X.-S. Wang, L. Wang, *Macromolecules* **2016**, *49*, 15 – 22; c) C. Cai, J. Lin, T. Chen, X. Tian, *Langmuir* **2010**, *26*, 2791 – 2797.

[11] a) I. Uematsu, Y. Uematsu, *Adv. Polym. Sci.* **1984**, *59*, 37 – 74; b) Y. Ishimura, F. Hamada, A. Nakajima, *Macromolecules* **1978**, *11*, 382 – 387; c) C.-J. Huang, F.-C. Chang, *Macromolecules* **2008**, *41*, 7041 – 7052.

[12] G. Maurstad, B. T. Stokke, *Curr. Opin. Colloid Interface Sci.* **2005**, *10*, 16 – 21.

[13] a) S. Lin, N. Numasawa, T. Nose, J. Lin, *Macromolecules* **2007**, *40*, 1684 – 1692; b) C. Cai, Y. Li, J. Lin, L. Wang, S. Lin, X.-S. Wang, T. Jiang, *Angew. Chem. Int. Ed.* **2013**, *52*, 7732 – 7736; *Angew. Chem.* **2013**, *125*, 7886 – 7890; c) G. K. Bourov, A. Bhattacharya, *J. Chem. Phys.* **2003**, *119*, 9219 – 9225.

Manuscript received: February 26, 2017
Final Article published: April 13, 2017

